Synthesis of PDMS- b -POEGMA Diblock Copolymers and Their Application for the Thermoresponsive Stabilization of Water-Supercritical Carbon Dioxide Emulsions

Pierre Legout, Guillaume Lefebvre, Marie Bonnin, Jean-Christophe Gimel, Lazhar Benyahia, Olivier Colombani, Brice Calvignac

Synthesis of PDMS-*b*-POEGMA diblock copolymers and their application for the thermo-responsive stabilization of water-supercritical carbon dioxide emulsions

Pierre Legout[1,2], Guillaume Lefebvre[1], Marie Bonnin[1], Jean-Christophe Gimel[1], Lazhar Benyahia[2], Olivier Colombani[2,] and Brice Calvignac[1,*]*

[1]Micro et Nanomédecines Translationnelles, MINT, UNIV Angers, UMR INSERM 1066, UMR CNRS 6021, Angers.

[2]Institut des Molécules et Matériaux du Mans (IMMM), UMR 6283 CNRS Le Mans Université, Avenue Olivier Messiaen, 72085 Le Mans Cedex 9, France.

KEYWORDS. supercritical carbon dioxide, emulsion, amphiphilic block copolymer, surfactant, poly(dimethyl siloxane), poly(ethylene glycol methacrylate), interfacial tension, stimuli-responsive.

Corresponding Authors

* olivier.colombani@univ-lemans.fr; brice.calvignac@univ-angers.fr

List of the number of pages, figures, and tables in Supporting Information

Number of pages: 17

Number of figures: 10

Number of tables: 4

Brief list of the contents in Supporting Information

1. Optimization of the conditions for the synthesis of $PDMS_{13}$-CTA;
2. Efficiency of the $PDMS_{13}$-CTA
3. Synthesis and characterization of $PDMS_{13}$-*b*-$POEGMA_5$
4. Determination of the cloud point pressure in CO_2 and of the cloud point temperature in water
5. γ measurements
6. Investigation of the aqueous phase before and after emulsification

1. Optimization of the conditions for the synthesis of $PDMS_{13}$-CTA

In order to optimize the conditions for the synthesis of $PDMS_{13}$-CTA from $PDMS_{13}$-OH (see Figure 3), different conditions were tested. The reaction was first conducted at rather low concentration with only a 1.2 excess of CTA-COOH relative to PDMS-OH (entry 1, table S1). In these conditions, a large amount of residual PDMS-OH was still present after 72 h, showing that the reaction was not complete. Increasing the excess of CTA-COOH and DCC to 5 eq. without changing the concentration of PDMS-OH nor the reaction time still resulted in a large amount of residual PDMS-OH after 72 h (entry 2). On the contrary, full conversion could be achieved even after only 24h by increasing the PDMS-OH concentration while keeping the excess of CTA-COOH and DCC at 5 eq. (entry 3). The concentration of the reaction medium was then further adjusted to limit the excess of CTA-COOH and DCC required for full consumption of PDMS-OH within 24 h (compare entries 4-6). Entry 6 corresponds to the optimal conditions among the different trials.

Table S1. Optimization of the PDMS-CTA synthesis at room temperature in dichloromethane.

	Molar ratio of PDMS-OH : CTA-COOH : DCC : DMAP	[PDMS-OH] mol/L	Reaction time	% residual PDMS-OH[a]
1	1 eq : 1.2 eq : 1eq : 0.12 eq	$2.8 * 10^{-2}$	72 h	50%
2	1 eq : 5 eq : 5 eq : 0.5eq	$2.8 * 10^{-2}$	72 h	30%
3	1 eq : 5 eq : 5 eq : 0.5 eq	$4.6 * 10^{-2}$	24 h	n. d.
4	1 eq : 1.5 eq : 1.5 eq : 0.2 eq	$2.8 * 10^{-2}$	24 h	25%
5	1 eq : 1.5 eq : 1.5 eq : 0.15 eq	$4.6 * 10^{-2}$	24 h	12%
6	1 eq : 1.5 eq : 1.5 eq : 0.15 eq	$22 * 10^{-2}$	24 h	n. d.

[a] Determined by ^{1}H NMR on the raw reaction medium. n.d. = not detected.

2. Efficiency of the $PDMS_{13}$-CTA

Figure S1 presents the refractive index response of the SEC for the polymers before (a) and after (b) purification. The residual PDMS-CTA cannot be seen with this detection because PDMS is isorefractive of THF (dn/dc ~ 0 mL/g).

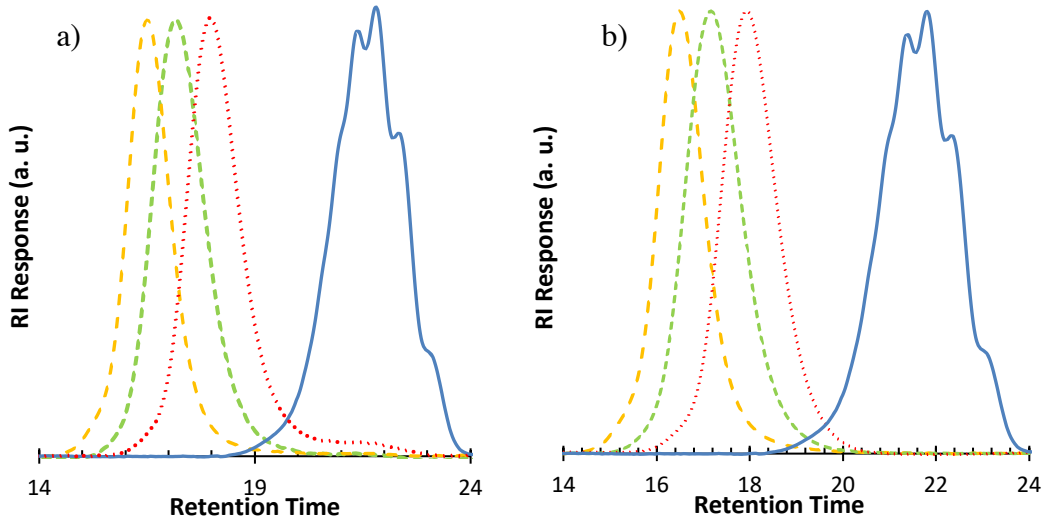

Figure S1. Size exclusion chromatograms of the first block $PDMS_{13}$-CTA (–) and of the diblock $PDMS_{13}$-*b*-$POEGMA_x$ (DP_n = 16 ···, DP_n = 31 – –, DP_n = 46 – ·) a) before and b) after purification by selective precipitation in pentane/diethyl ether (80/20 v/v).

In order to determine the efficiency of the PDMS-CTA from the SEC chromatograms obtained using UV detection (Figure 5a), the molar extinction coefficient (ε) of the $PDMS_{13}$-CTA and of the $PDMS_{13}$-*b*-$POEGMA_x$ at 254 nm was first determined by measuring the absorbance (A) at 254 nm of solutions of these polymers in THF at different concentrations (C) by UV-visible spectroscopy. The measurements were conducted in l = 1 cm cuvettes and ε was deduced using Beer-Lambert law (Eq. S1), see Figure S2.

$$A = \varepsilon l c \qquad \text{Equation S1}$$

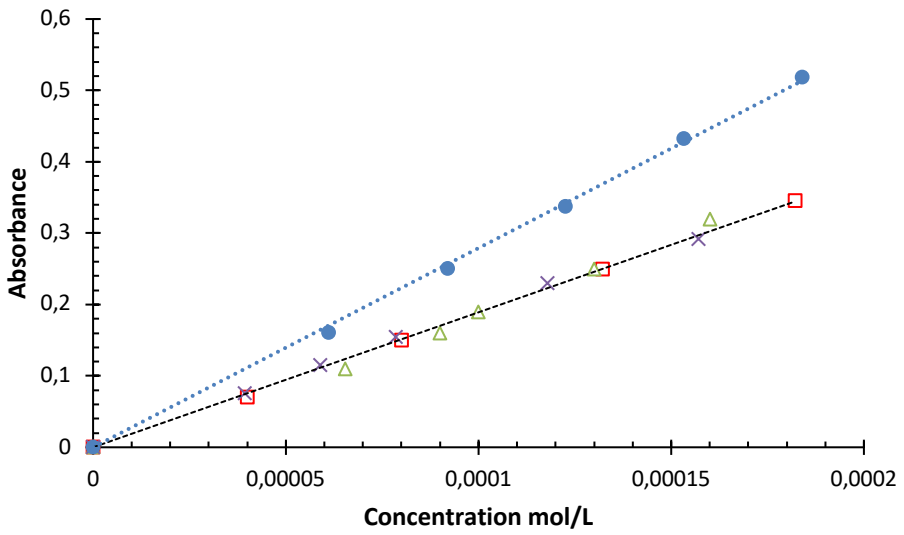

Figure S2. Evolution of the absorbance at 254 nm for different concentrations of $PDMS_{13}$-CTA (●), $PDMS_{13}$-*b*-$POEGMA_{46}$ (□), $PDMS_{13}$-*b*-$POEGMA_{31}$ (△) and $PDMS_{13}$-*b*-$POEGMA_{16}$ (x).

The CTA efficiency was evaluated according to Eq. S2, where $A_{PDMS\text{-}CTA}$ and $A_{PDMS13\text{-}b\text{-}POEGMAx}$ correspond to the respective areas of the residual $PDMS_{13}$-CTA and of the $PDMS_{13}$-*b*-$POEGMA_x$ peaks on the SEC chromatograms (UV-detection) of the crude polymer before precipitation and $\varepsilon_{PDMS\text{-}CTA}$ and $\varepsilon_{PDMS13\text{-}b\text{-}POEGMAx}$ correspond to their respective ε values.

$$\text{CTA efficiency} = \frac{\frac{A_{PDMS-b-POEGMA}}{\xi_{PDMS-b-POEGMA}}}{\frac{A_{PDMS-CTA}}{\xi_{PDMS-CTA}} + \frac{A_{PDMS-b-POEGMA}}{\xi_{PDMS-b-POEGMA}}} \qquad \text{Equation S2}$$

3. Synthesis and characterization of $PDMS_{13}$-*b*-$POEGMA_5$

The synthesis of a $PDMS_{13}$-*b*-$POEGMA_5$ diblock was attempted with a [monomer]:[CTA]:[AIBN] molar ratio of 20:1:0.2 and with a final conversion of ~25%, all other conditions being the same as for the other diblocks. Figure S3 indicates that the concentration of radicals was constant throughout the polymerization. However, Figure S4a clearly indicates that the crude diblock copolymer contained a large amount of residual PDMS-CTA. Purification was attempted by precipitating the polymer in different solvents in order to remove both residual

OEGMA and PDMS-CTA. The polymer did precipitate in water/methanol (20/80 v/v) and diethyl ether/methanol (80/20, 90/10, 95/5 v/v) where OEGMA was miscible. Nevertheless, OEGMA was not efficiently removed by precipitation in these solvent mixtures. Dialysis (Cellulose, 1000 MWCO, Spectrum) in water for one week was conducted and afforded complete removal of residual OEGMA. Precipitation in pentane and toluene/diethyl ether (80/20 v/v) which were good solvents for PDMS-CTA was attempted, but the polymer did not precipitate in these solvents. Precipitation was finally achieved in pentane/diethyl ether (80/20 v/v), but it did not allow removal of PDMS-CTA (see Figure S4). The POEGMA block was most certainly too short to result in a sufficient difference of solubility between the $PDMS_{13}$-CTA and the $PDMS_{13}$-*b*-$POEGMA_5$ diblock, explaining the inefficiency of the purification.

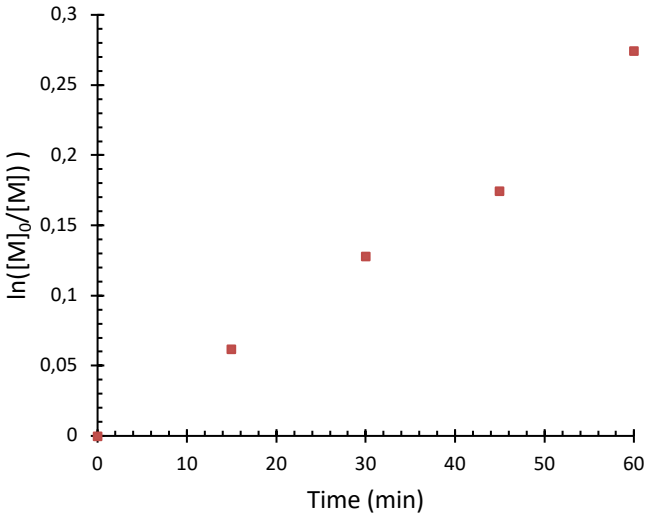

Figure S3. Evolution of $\ln([M]_0/[M]) = f(t)$ during the synthesis of $PDMS_{13}$-b-$POEGMA_5$. See conditions in the text.

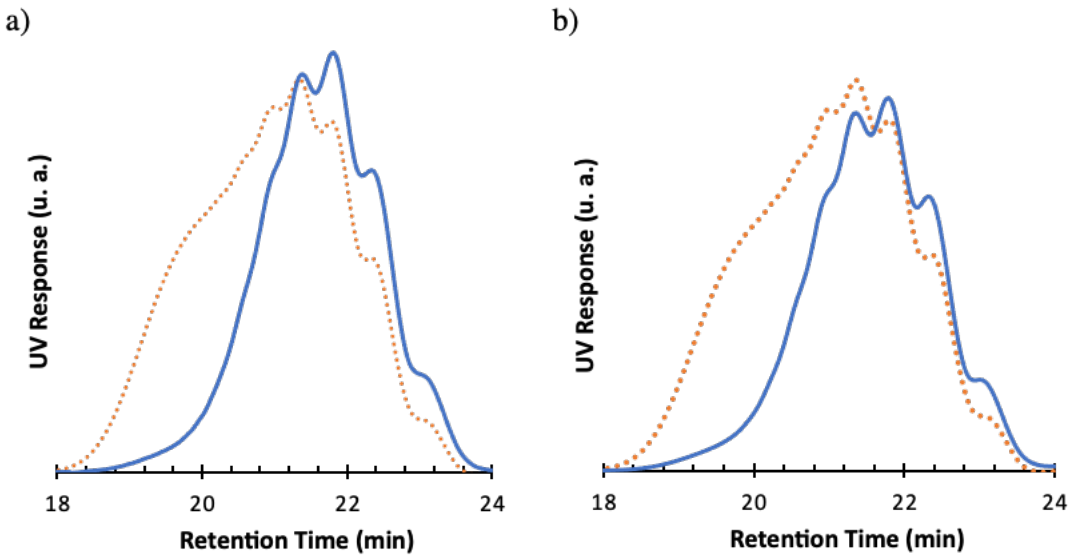

Figure S4. Size exclusion chromatograms of the macroCTA ($PDMS_{13}$-CTA, –) and of the $PDMS_{13}$-*b*-$POEGMA_5$ diblock (···) a) before purification, and b) after purification by dialysis in water and precipitation in pentane/diethyl ether (80/20 v/v).

4. Determination of the cloud point pressure in CO_2 and of the cloud point temperature in water

Cloud point pressures of the polymers in $scCO_2$

Cloud point pressures were obtained for the diblock copolymers and for their constituting homopolymeric blocks by analyzing grey intensity: $P_{c(0)}$ and $P_{c(i)}$ of three samples at 40°C. Typical curves for the diblock copolymers are represented on Figure S5.

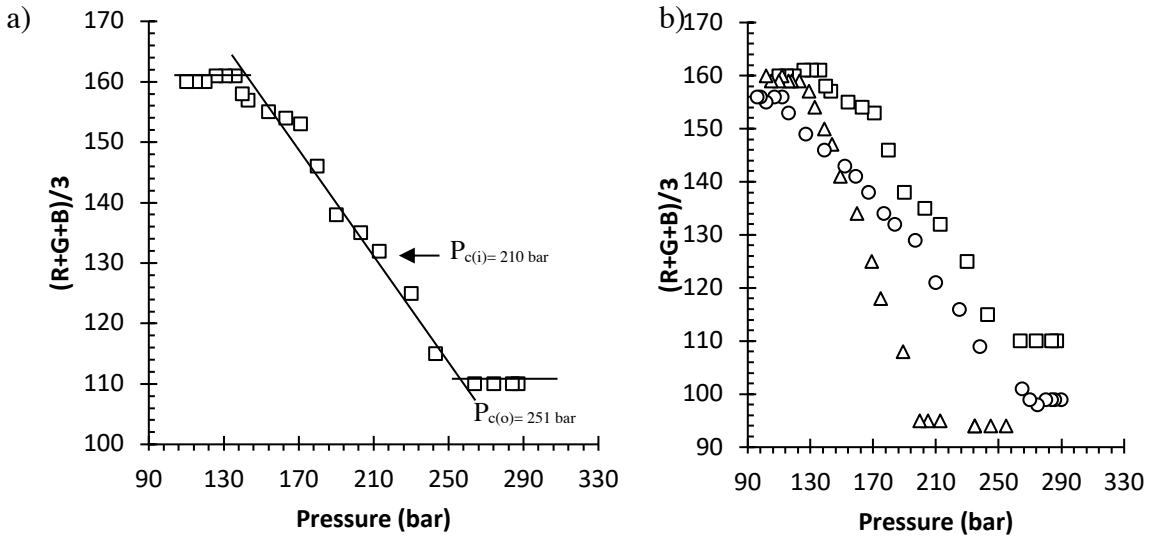

Figure S5. a) Variation of (R+G+B)/3 intensities with pressure for a depressurization speed of 10 bar/min at 40°C for $PDMS_{13}$-*b*-$POEGMA_{46}$ (0.5 % w/v) in $scCO_2$. $P_{c(0)}$ and $P_{c(i)}$ correspond to the cloud point pressure respectively at the onset of the increase of turbidity or at the inflexion point. b) Variation of (R+G+B)/3 with pressure, for a depressurization speed of 10 bar/min at 40°C for $PDMS_{13}$-*b*-$POEGMA_x$ (0.5 % w/v) (DP_n = 16 (△), DP_n = 31 (○), DP_n = 46 (□)) in $scCO_2$.

$P_{c(i)\ PDMS13\text{-}b\text{-}POEGMA46}$: 210 bar, $P_{c(i)\ PDMS13\text{-}b\text{-}POEGMA31}$: 180 bar, $P_{c(i)\ PDMS13\text{-}b\text{-}POEGMA16}$: 150 bar

The cloud point was not measured at 80°C. However, the diblock copolymers should be soluble at this temperature at least according to the cloud point pressures determined at 40°C for entropic reasons.

Cloud point temperature of the diblock copolymers in water

$PDMS_{13}$-*b*-$POEGMA_x$ copolymers were solubilized in water at room temperature at different concentrations (0.1; 0.5 and 1 % w/v). After dissolution (~20 min), their thermosensitive behavior was studied in water at atmospheric pressure and determined by turbidimetry using transmitted light measurements (Turbiscan Tower, Formulaction, Toulouse, France). 15 mL of aqueous

polymer solutions were placed in 30 mL vials. Turbiscan analyses were carried out from 25 to 80°C at a heating rate of 0.9°C/min with one transmittance measurement every 60 s. The samples were scanned from the bottom to the top by a near infrared light source (λ = 880 nm), and the transmitted light signal was collected. These data were used to detect the appearance of the turbidity and thus the cloud point temperature (T_{CP}) when the copolymer starts to precipitate due to the LCST of the POEGMA block. The cloud point temperature in water was calculated at the fall of the transmittance (Figure S6).

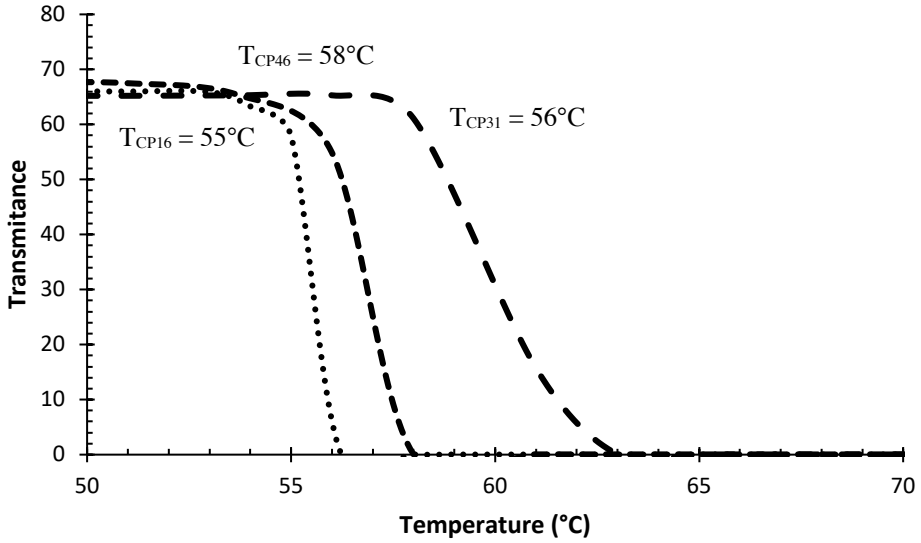

Figure S6. Variation of Transmittance with pressure with a heating rate of 0.9°C/min for $PDMS_{13}$-*b*-$POEGMA_x$ ($x = 16$ ···, $x = 31$ - -, $x = 46$ **--**) in water.

5. γ measurements

γ was measured at different concentrations (Table S2) and pressures (Table S3), and the difference between γ without polymer and γ with polymer, called surface pressure (π), was observed as a function of CO_2 density at different temperatures (Figure S7).

Table S2. γ as a function of the weight-concentrations of $PDMS_{13}$-*b*-$POEGMA_x$ at 40°C, 250 bar and for different *x* values (3 trials).

	***x* = 16 (mN/m)**	***x* =31 (mN/m)**	***x* = 46 (mN/m)**	**Without polymer**
C = 0.1 % w/v	2.1; 2.5; 2.3	2.1; 1.9; 2.1	3.5; 3.0; 3.9	25.2; 24.6; 23.3
C = 0.5 % w/v	2.1; 1.9; 2.1	1.5; 1.6; 1.6	4.0; 3.9; 4.0	
C = 1.0 % w/v	1.5; 1.6; 1.4	1.3; 1.2; 1.2	2.1; 2.2; 2.3	

Table S3. γ measurements at 40°C, different pressures, without polymer or with 1 % w/v of $PDMS_{13}$-*b*-$POEGMA_x$ (different *x* values) in the aqueous phase (3 trials).

	***x* = 16 (mN/m)**	***x* = 31 (mN/m)**	***x* = 46 (mN/m)**	**Without polymers**
P = 100 bar	4.0; 3.9; 4.0	6.0; 6.1; 6.5	9.2; 9.7; 9.5	32.2; 33.4; 35.0
P = 150 bar	2.4; 2.1; 2.3	2.4; 2.4; 2.3	6.6; 7.1; 6.9	27.3; 29.8; 27.7
P = 200 bar	1.7; 1.8; 2.0	1.7; 1.6; 1.7	4.9; 4.7; 4.2	26.8; 26.6; 25.1
P = 250 bar	1.5; 1.6; 1.4	1.3; 1.2; 1.2	2.1; 2.2; 2.3	25.2; 24.6; 23.3

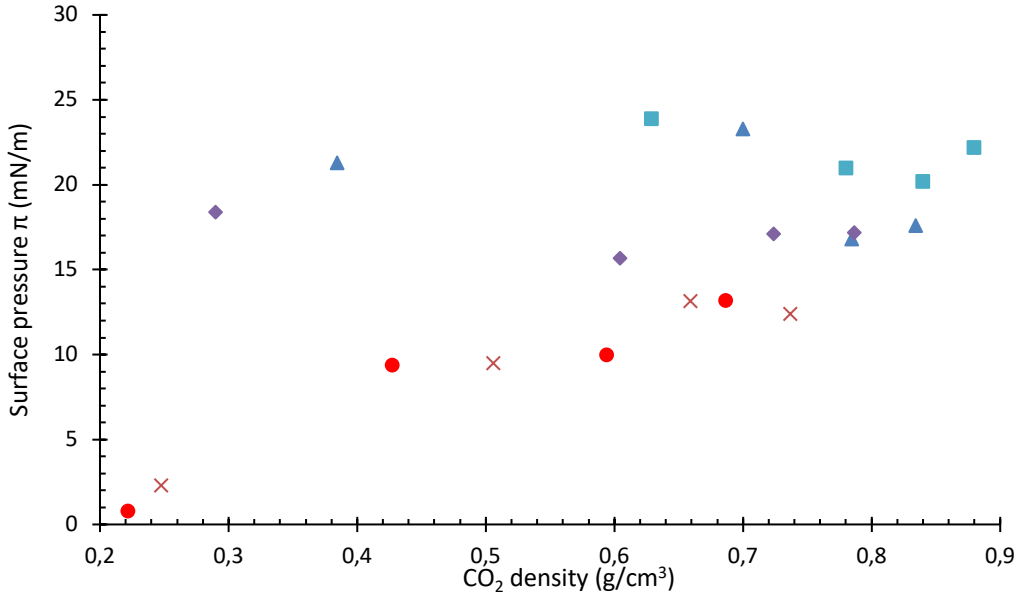

Figure S7. Surface pressure π as a function of CO_2 density at different temperatures = 40°C (■), 50°C (▲), 60°C (◆), 70°C (x) and 80°C (●) with 1% $PDMS_{13}$-*b*-$POEGMA_{46}$

Figure S7 shows that increasing the temperature causes a decrease of the surface pressure π and reveals that at 40°C and 50°C, π remains rather low and barely depends on the CO_2 density.

6. Investigation of the aqueous phase before and after emulsification

DLS measurements were first performed to characterize the $PDMS_{13}$-*b*-$POEGMA_{46}$ in water at 20°C and 1 bar after a 0.1 μm filtration in very clean glass vials. A multi-angle DLS device was used (LS spectrometer equipped with a 500 mW, 660 nm laser, LS Instruments AG). A 1% w/v polymer solution was prepared and had to be diluted below 0.5% w/v to suppress a very small amount of multiple scattering. No angular dependency was observed (from 20° to 150°) and a z-average hydrodynamic radius close to 10 nm with a polydispersity index close to 0.05 were measured at any angle. This evidenced the formation of rather monodisperse micellar structures in water at 20°C and ambient pressure. CryoTEM of $PDMS_{13}$-*b*-$POEGMA_{31}$ was conducted with a 1

% w/v aqueous solution of the polymer (Figure S8), confirming the formation of spherical micelles with dimensions compatible with those determined by DLS with the multi-angle apparatus.

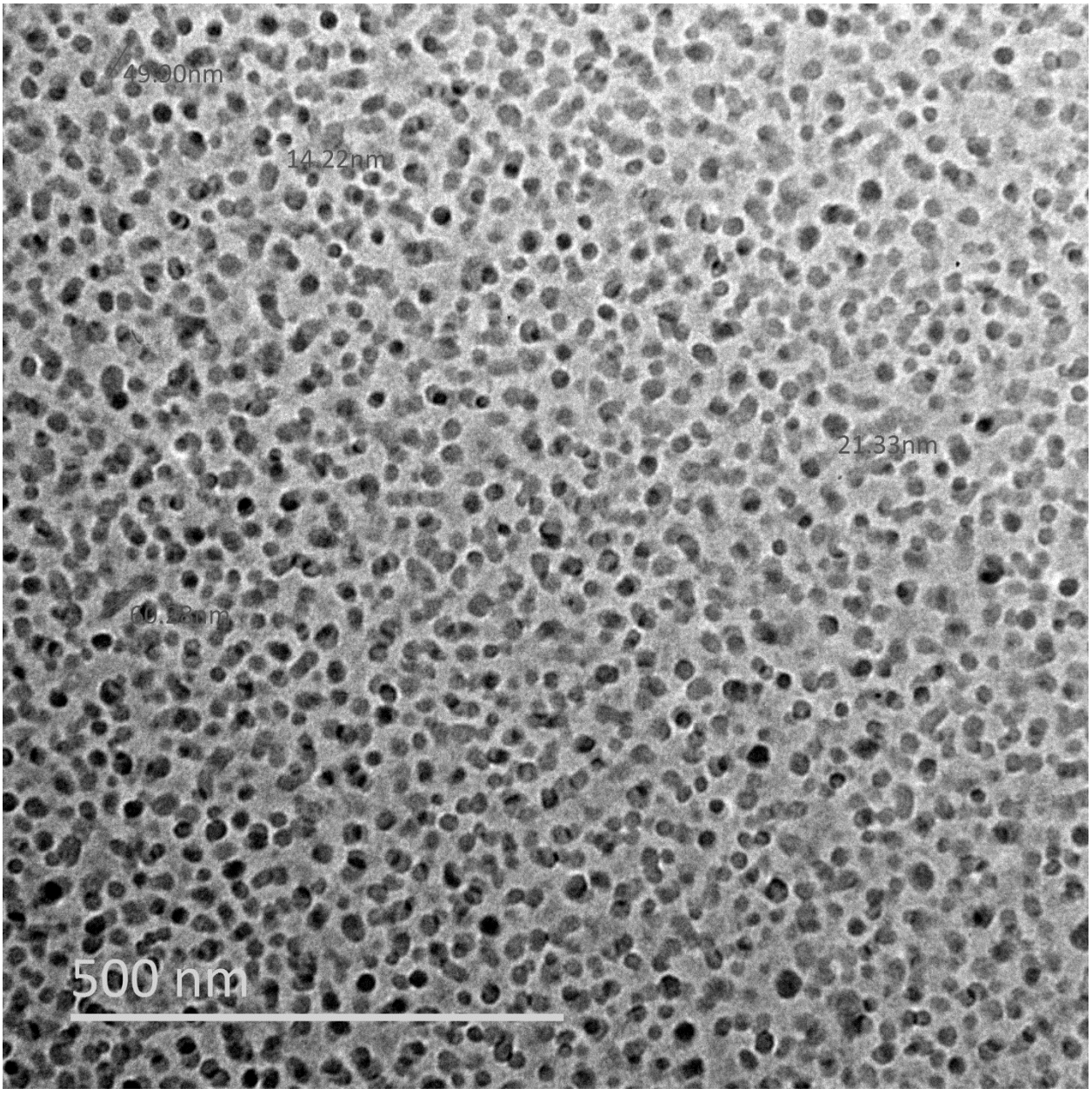

Figure S8. CryoTEM of $PDMS_{13}$-*b*-$POEGMA_{31}$ in water at 1 % w/v. The experiment was carried out on a 2100 HR microscope (Jeol) running at 120 kV equipped with a LaB6 filament. Specimens for cryoTEM observations were treated using a cryo-plunge 3 system (Gatan) in which a drop of

the aqueous solution was deposited onto glow-discharged carbon-coated grids (Agar Scientific). The TEM grid was then blotted so that a thin liquid layer was formed spanning across the holes of the supporting carbon film. The grid was quickly plunged into liquid ethane cooled by liquid nitrogen to vitrify the liquid film. The vitrified specimens were put in a cryo-transfer specimen holder (626, Gatan) cooled with liquid nitrogen. The samples were observed at −176°C and recorded with a 2048 × 2048 ORIUS SC200D CCD camera (Gatan). This figure was treated with the software Fiji.

DLS measurements were then performed with the remote head of a VASCO Kin DLS (Cordouan®) apparatus with a 638 nm laser at 170° angle through the observation window of the home-made device (Figure 2), allowing investigation of the aqueous phase under pressure before and after emulsification (Figure S9). We stress that these experiments could not be conducted in the same extreme conditions of cleanliness as those conducted at room temperature because the solutions had to be introduced in the home-made device. Before emulsification, the aqueous $PDMS_{13}$-*b*-$POEGMA_x$ diblock copolymer solution was measured at 1 % w/v, 100 bar and 40°C (Figure S9) for the three *x* values. The apparent hydrodynamic radii extracted from the auto-correlation functions using the cumulant algorithm[1] were significantly higher than those determined with the multi-angle apparatus at 20°C and 1 bar (see Table S4). A more appropriate SBL algorithm (Sparse Baysin Learning)[2] resulted into two populations (see Table S4): one corresponding to small scatterers with sizes compatible with those determined by multi-angle DLS or cryoTEM and with the formation of polymeric micelles, and the other corresponding to much larger aggregates. The latter significantly contributed to the scattered intensity because of their size but correspond to a very small amount of material. Otherwise, they would indeed have

overwhelmed the DLS signal and the small micelles would not have been detected.[3] This low amount of larger aggregates were probably ill-defined aggregates of polymer or aggregates of polymer micelles which are often observed for amphiphilic copolymers in aqueous medium.[3] They could be eliminated by filtration on 0.1 μm filters for the experiments conducted at 20°C and 1 bar but could not be avoided for the experiments under pressure in the home-made device were the same high quality handling of the samples was not possible.

Table S4. Intensity of the scattered light in the aqueous phase of the $PDMS_{13}$-*b*-$POEGMA_x$ diblock copolymer (1% w/v, 100 bar, 40°C) before any emulsification.

DP_n (POEGMA)	R_h (nm)
$x = 16$	Cumulant[a]: 66 nm SBL[b]: 28 nm (6%); 82 nm (94%)
$x = 31$	Cumulant: 23 nm SBL = 9 nm (38%); 54 (62%)
$x = 46$	Cumulant = 23 nm SBL = 15 nm (31%); 65 nm (69%)

[a] The Cumulant analysis[1] is based on a Taylor expansion of the correlogram at small delay times. It only gives access to the two first moments of the scatterer distribution and no information is given about the shape of the distribution, [b] The SBL algorithm[2] is based on an inverse Laplace transform (ILT) of the correlogram. ILT methods are very sensitive to the noise in the data and usually give many spurious pics to minimize the square error. The SBL algorithm proposes a new regularization technique that limits this number of pics. In any case the accurate position of a pic depends on its contribution to the scattered intensity (the bigger, the better).

In spite of the presence of these larger aggregates in the DLS experiments conducted directly in the home-made device, the auto-correlation functions obtained for the aqueous polymer phase before emulsification were compared with those of the aqueous phase after emulsification and creaming (Figure S9). The data have been normalized on Figure S9 to get rid of the difference in

intercept allowing an easier comparison of the curves. In most cases, it appears that the dimensions of the scatterers were much larger after emulsification and creaming than before. In these cases, any strong variation of the scattered intensity could only be due to a strong decrease of the polymer concentration in the aqueous phase after emulsification and creaming as explained in the manuscript. For $PDMS_{13}$-*b*-$POEGMA_{31}$ at 150 and 200 bar and for $PDMS_{13}$-*b*-$POEGMA_{46}$ at 250 bar, DLS revealed a small shift of the auto-correlation functions towards shorter times after emulsification and creaming (see Figure S9). This was attributed to a decrease of the small amount of the large ill-defined aggregates initially present before emulsification, as confirmed for $PDMS_{13}$-*b*-$POEGMA_{31}$ (see Figure S10). In that case, the decrease of the scattered intensity is a combination of the decrease of the polymer concentration and the scatterer size. In these circumstances, the relative polymer concentration is probably higher than the relative scattered intensity indicated in Table 4, as mentioned in the manuscript.

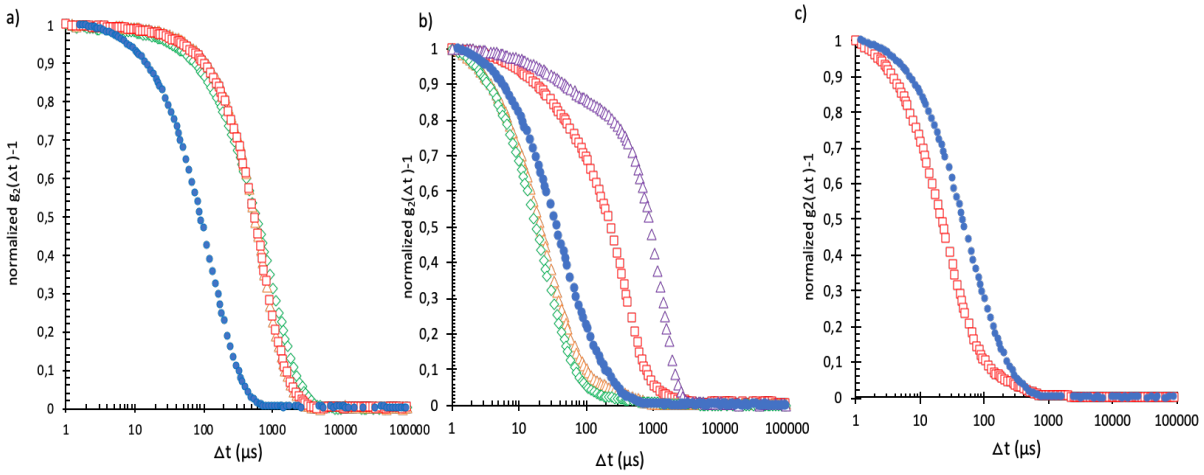

Figure S9. Normalized DLS correlograms of the aqueous polymer phase before emulsification (●) at 100 bar and of the bottom aqueous phase after emulsification and creaming for a water/$scCO_2$ 50/50 v/v ratio in the presence of $PDMS_{13}$-*b*-$POEGMA_x$ (0.5 % w/v polymer with

respect to the total volume, corresponding to 1 % w/v in the initial aqueous phase). With a) $PDMS_{13}$-*b*-$POEGMA_{16}$, b) $PDMS_{13}$-*b*-$POEGMA_{31}$, c) $PDMS_{13}$-*b*-$POEGMA_{46}$ at different pressures 100 bar (△), 150 bar (◇), 200 bar (△), 250 bar (□) and 40°C. The DLS correlogram for $PDMS_{13}$-*b*-$POEGMA_{16}$ at 100 bar after emulsification and creaming is not shown because the scattered intensity was too low to obtain a reliable correlogram. The DLS correlograms for $PDMS_{13}$-*b*-$POEGMA_{46}$ at 100-200 bar after emulsification are not presented because the aqueous phase was too turbid (Figure 8d) due to multiple light-scattering.

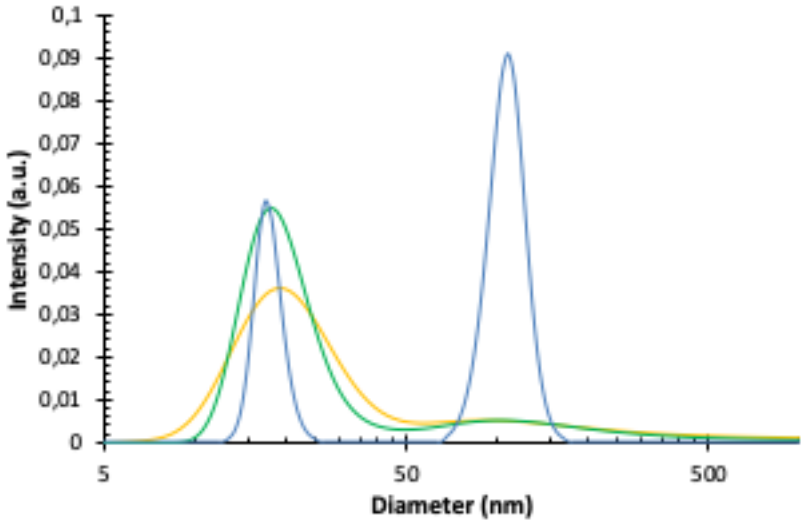

Figure S10. DLS intensity-weighted size distribution curves (obtained using the SBL algorithm) of the aqueous polymer phase before emulsification (–) at 100 bar and of the bottom aqueous phase after emulsification and creaming for a water/$scCO_2$ 50/50 v/v ratio in the presence of $PDMS_{13}$-*b*-$POEGMA_{31}$ (0.5 % w/v polymer with respect to the total volume, corresponding to 1 % w/v in the initial aqueous phase) at 40°C and different pressures: 150 bar (–) and 200 bar (–).

Supplementary References

(1) Koppel, D. E. Analysis of Macromolecular Polydispersity in Intensity Correlation Spectroscopy: The Method of Cumulants. *J. Chem. Phys.* **1972**, *57* (11), 4814–4820. https://doi.org/10.1063/1.1678153.

(2) Nyeo, S.-L.; Ansari, R. R. Sparse Bayesian Learning for the Laplace Transform Inversion in Dynamic Light Scattering. *J. Comput. Appl. Math.* **2011**, *235* (8), 2861–2872. https://doi.org/10.1016/j.cam.2010.12.008.

(3) Patterson, J. P.; Robin, M. P.; Chassenieux, C.; Colombani, O.; O'Reilly, R. K. The Analysis of Solution Self-Assembled Polymeric Nanomaterials. *Chem. Soc. Rev.* **2014**, *43* (8), 2412–2425. https://doi.org/10.1039/C3CS60454C.